Nuclear Instruments and Methods in Physics Research A304 (1991) 673–678
North-Holland

A scheme for XUV generation based on a laser-pumped FEL with an axial electric field

M. Cohen, A. Gover and S. Ruschin

Faculty of Engineering, Tel-Aviv University, Ramat-Aviv 69978, Israel

A scheme for an XUV-wavelength free electron laser based on trapping electrons in a laser beat in the presence of an axial accelerating electric field and operating in a continuous pulse train (regenerative amplifier) mode is proposed. Some examples are shown based on ring optical resonator designs for both the wiggler and the signal radiation. The signal radiation is in a spectral region of tens of nanometers. A calculation of the parameters indicates that the technology required for an experiment is within the state of the art. Examples presented are based on a pump (wiggler) field produced by a continuously pulsed CO_2 or Nd:YAG laser and a continuous train of sub-ns electron beam pulses in the 0.4–2 MeV range. The signal builds up from an injected single pulse, which can be generated by high-harmonic (third, fifth) multiplication in the gas of a doubled (tripled) Nd:YAG laser or an excimer laser. The proposed scheme thus converts a single pulse of XUV radiation into a continuous train of pulses with high average power in the same wavelength region.

1. Introduction

In the last decade, a substantial research and development effort has been made to attain a free electron laser operating at a short wavelength (below UV) [1–6]. The main impediment for an FEL operating at a short wavelength is the limited quality of the electron beam which makes it difficult to meet the stringent energy spread and emittance acceptance parameters at short wavelengths.

In this article we propose to modify the XUV Compton scattering regenerative amplifier scheme suggested by Gea-Banacloche et al. [1,2] and operate it in the nonlinear regime with an axial electric field as proposed earlier by Gover et al. [7]. In this operation mode, the electrons are trapped in a laser beat and an axial electric field to enhance the gain. Since this scheme is based on operation in the nonlinear regime, the electron beam axial velocity spread acceptance is limited only by the depth of the beat wave (ponderomotive) potential well and not by the wiggler length (as in the linear regime [1,2]). This can help to obtain higher electron beam acceptance parameters and more favorable design parameters. The use of a laser wiggler makes it possible to realize an XUV source with a low-energy compact accelerator. Our particular scheme requires injection of a single pulse of XUV radiation in order to start oscillation, but then a continuous train of XUV radiation pulses is produced. This scheme is shown in fig. 1.

2. Theory

In order to calculate the forces applied on an electron, we use the formulation of ref. [7]. The pump and the signal radiation fields are

$$\boldsymbol{E}_w(\boldsymbol{r}, t) = \mathrm{Re}\left[\tilde{\boldsymbol{E}}_w \, \mathrm{e}^{-\mathrm{i}(\omega_w t + k_w z)}\right], \quad (1)$$

$$\boldsymbol{E}_s(\boldsymbol{r}, t) = \mathrm{Re}\left[\tilde{\boldsymbol{E}}_s \, \mathrm{e}^{-\mathrm{i}(\omega_s t - k_s z)}\right], \quad (2)$$

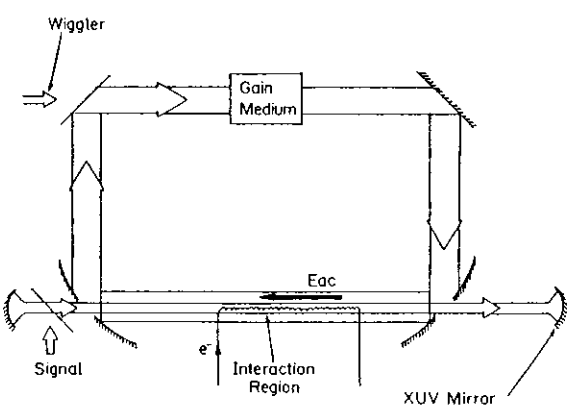

Fig. 1. A proposed scheme for an XUV-wavelength FEL consists of a Fabri–Perot resonator for the signal and a matched ring optical resonator for the pump. It includes means (an optical switch) for injecting the signal radiation into the signal resonator and an amplifier in the pump resonator to compensate for losses in the pump power.

0168-9002/91/$03.50

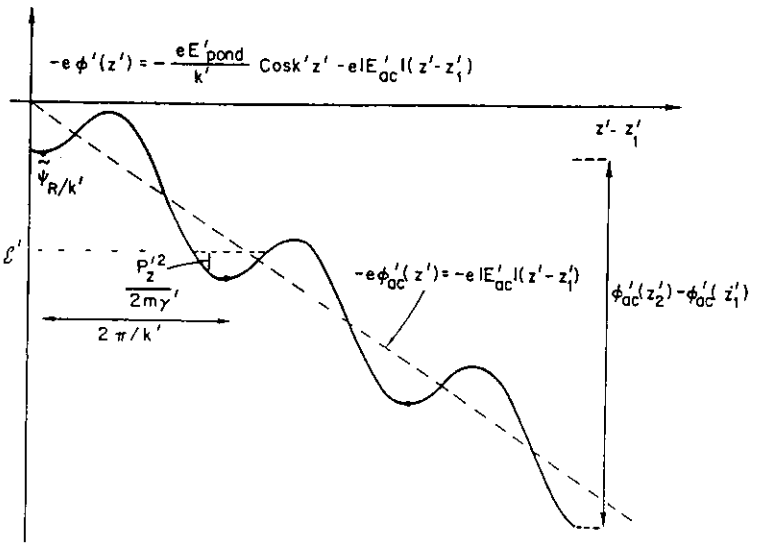

Fig. 2. The energy diagram of the ponderomotive potential in the presence of an accelerating electric field.

where $\tilde{E}_w$, $\tilde{E}_s$, ω_w, ω_s, k_w and k_s, are the complex amplitudes, the frequencies and the wave numbers of the pump (wiggler) and signal radiations. The fields given in eqs. (1) and (2) are assumed to be transverse fields, independent of the transverse coordinates. These waves are propagating in opposite directions and overlap in the interaction region, as shown in fig. 1. The electron pulse is traveling in the same direction as the signal. The equation which describes the motion of a single electron in the ponderomotive field of the two waves in the presence of an axial accelerating electric field, is the axial force equation [7]:

$$\frac{dp_z}{dt} = -eE_{pond}\sin(kz-\omega t) - eE_{ac}, \tag{3}$$

where $\omega = \omega_s - \omega_w$, $k = k_s + k_w$, E_{ac} is the externally applied axial electric field and E_{pond} is the ponderomotive field amplitude given by

$$E_{pond} = \frac{e}{4\pi\gamma_0 mc^2}(\lambda_s+\lambda_w)\left|\tilde{E}_s^* \cdot \tilde{E}_w\right|, \tag{4}$$

where λ_s and λ_w are the wavelengths of the signal and pump, respectively. e and m are the charge and rest mass of the electron, respectively, and c is the speed of light. γ_0 is the relativistic Lorentz factor defined by

$$\gamma_0 = \frac{1}{\sqrt{1-(v/c)^2}}, \tag{5}$$

where v is the mean velocity of the electron beam.

The electrons travel with an axial velocity component close to the phase velocity of the ponderomotive wave $v_z \simeq v_{ph}$ where the phase velocity v_{ph} is

$$v_{ph} = \frac{\omega_s - \omega_w}{k_s + k_w} = \left(\frac{\lambda_w - \lambda_s}{\lambda_w + \lambda_s}\right)c. \tag{6}$$

In the reference frame moving with the velocity of the ponderomotive wave phase, a synchronous electron will have zero kinetic energy. If an electron gets trapped and keeps in phase with the ponderomotive wave, no kinetic energy will be added to the electrons, despite the accelerating axial field E_{ac}.

In order to keep the electrons trapped in the ponderomotive potential wells, three conditions must be satisfied [7]. First,

$$E_{ac} \ll E_{pond}. \tag{7}$$

The accelerating electric field must be small enough. If the field will be too high, the potential wells will be tilted strongly and thus trapping will not occur. The energy diagram of the ponderomotive potential with an applied accelerating electric field is given in fig. 2.

Second, the axial energy spread in the electron beam, $\Delta\mathcal{E}$, has to be small compared to the energy depth (trough to peak) of the potential wells. Electrons which have energies substantially different from the resonance energy, γ_{ph}, cannot get trapped and just experience free space acceleration due to E_{ac}. This trapping condition was derived in ref. [7] and is given by

$$\Delta\mathcal{E} \ll \mathcal{E}_{trap} = 2\sqrt{2}\,\beta_{0z}\gamma_{0z}ce\left(\frac{\left|\tilde{E}_w \cdot \tilde{E}_s^*\right|}{\omega_w\omega_s}\right)^{1/2}, \tag{8}$$

we define $\beta_{0z} = v_{0z}/c$, where $v_{0z} = v_{ph}$ is the resonance velocity. γ_{0z} is an axial energy factor associated with the resonance factor γ_0, as follows:

$$\gamma_{0z} = \frac{\gamma_0}{1+a^2}, \tag{9}$$

where a is the normalized transverse vector potential of the radiation fields ($a = eA_\perp/mc$). It can be assumed to

be negligible, $a \ll 1$. In all practical cases, using the resonance condition $v_z = v_{ph}$ and eq. (6), γ_{0z} is given by

$$\gamma_{0z} \approx \frac{\lambda_w + \lambda_s}{2(\lambda_w \lambda_s)^{1/2}}, \tag{10}$$

and the required electron accelerator energy is

$$\delta_e = (\gamma_0 - 1)mc^2 = \left(\frac{\lambda_w + \lambda_s}{2(\lambda_w \lambda_s)^{1/2}} - 1\right)mc^2. \tag{11}$$

The third condition that must be satisfied in order to attain electron trapping is related to the longitudinal space charge field. This field, which is associated with the spatial bunching of the trapped electrons, should be negligible in comparison with the ponderomotive field,

$$E_{sc} = \left(\frac{\mu_0}{\epsilon_0}\right)^{1/2} \frac{J_{trap}}{\beta_{0z} k} \ll E_{pond}, \tag{12}$$

where J_{trap} is the current density of the trapped electrons.

The trapped electrons are seen in the laboratory frame to traverse at a constant phase velocity across the potential drop $\phi_{ac}(z_2) - \phi_{ac}(z_1)$, which is applied along the interaction length. If the electric accelerating field E_{ac} is constant in the interaction region, then this potential drop can be calculated by the value of the electric field multiplied by the interaction length, $E_{ac} \times l_{int}$. Since no kinetic energy is added to the trapped electrons, the potential energy which was released is transformed into radiation field energy, governed by the Maxwell's equations [8]. The gain of the FEL will be

$$G = \frac{\Delta P_s}{P_s} = \frac{I_{trap}(\phi_{ac}(z_2) - \phi_{ac}(z_1))}{P_s}, \tag{13}$$

where I_{trap} is the current intensity of the trapped electrons and P_s is the signal power. In this scheme the energy extraction is from the accelerating potential and not from the kinetic energy of the electron beam. Since it is difficult to get an appreciable single path gain in this scheme, we propose to use it in a regenerative amplifier configuration which will operate in a continuous pulse train mode. In this operation mode, a single pulse of moderate peak power can be converted into a train of pulses with high average power.

3. Parameter selection

In this section we will present the main parameters that characterize the FEL operating in the scheme which is described above. The parameters of this scheme will be selected for operating in the XUV region pulse train mode.

We first derive an expression for the interaction length along which the energy is extracted. For a reason that will be clarified in the next section it will be assumed that

$$\tau_w \ll \tau_s. \tag{14}$$

where τ_w and τ_s are the pulse durations of the pump and the signal, respectively. As is described in the previous section, the optical pulses which travel in opposite directions, propagate one through the other, while the electron pulse travels through the optical pulses' overlap region with a velocity $v_{0z} = v_{ph}$ in the same direction as the signal. According to the assumption (14), almost all the trapped electrons in a continuous electron beam will experience the same interaction time. The interaction time is defined as the time period in which the electron experiences the presence of both the pump and the signal field. This period of time, calculated in the laboratory frame, is given by

$$t_{int} = \frac{\tau_w}{1 + \beta_{0z}}. \tag{15}$$

Correspondingly, the interaction length, which is the distance that a trapped electron passes during the interaction time, can be expressed as follows:

$$l_{int} = \beta_{0z} c t_{int} = \frac{l_w}{1 + 1/\beta_{0z}}, \tag{16}$$

where $l_w = c\tau_w$ is the length of the pump pulse. In any case, where the Doppler shift is significant ($\lambda_s \ll \lambda_w$), it can be seen from eq. (6) that β_{0z} is close to unity. In such circumstances, the interaction time is half of the pump time duration τ_w and the signal and pump pulses will completely separate after a time equal to half the duration of pump pulse beam, the time the two pulses intersect.

We will derive the FEL parameters under the assumption that the waves which were given by the fields in eqs. (1) and (2) are Gaussian beams [9]. Diffraction of the long-wavelength pump wave constrains the effective interaction length to be of the order of a Rayleigh length. Since the interaction length was fixed by eq. (16), the Rayleigh length of the pump, z_{0w}, is selected as

$$z_{0w} = l_{int}/2. \tag{17}$$

With this adjustment, the pump field amplitude at $z = \pm z_{0w}$ will be reduced by a factor $\sqrt{2}$ compared to its value at the plane $z = 0$. The waist, w_{0w}, of the Gaussian pump beam is

$$w_{0w} = (z_{0w}\lambda_w/\pi)^{1/2}. \tag{18}$$

If the waist of the signal wave is focused to be equal to the waist of the pump wave, the signal field amplitude on the axis at the planes $z = \pm z_{0w}$ will decrease to

$$\tilde{E}_s(z = z_{0w}) = \frac{\tilde{E}_s(0)}{(1 + z_{0w}^2/z_{0s}^2)^{1/2}} = \frac{\tilde{E}_s(0)}{(1 + \lambda_s^2/\lambda_w^2)^{1/2}}. \tag{19}$$

where $\tilde{E}_s(0)$ is the amplitude of the signal field on the axis at the plane $z = 0$ and z_{0s} is the Rayleigh length of the signal. It is concluded from eq. (19) that when the wavelength of the signal is in the XUV region ($\lambda_s \ll \lambda_w$), the diffraction of the signal wave throughout the interaction length is entirely negligible. The amplitude of the pump electric field can be expressed in terms of the pulse power by integrating the intensity over the cross section of the Gaussian mode. This integration yields

$$|\tilde{E}_w(0)| = \frac{2}{w_{0w}}\left(\frac{\mu_0}{\epsilon_0}\right)^{1/4}\left(\frac{P_w}{\pi}\right)^{1/2}, \tag{20}$$

where P_w is the pump beam power. Similarly, we can write an expression for the amplitude of the signal electric field:

$$|\tilde{E}_s(0)| = \frac{2}{w_{0s}}\left(\frac{\mu_0}{\epsilon_0}\right)^{1/4}\left(\frac{P_s}{\pi}\right)^{1/2}, \tag{21}$$

where P_s is the signal beam power. The pulse energy is assumed to be $\mathscr{E}_{w,s} = P_{w,s} \times \tau_{w,s}$.

In order to express the ponderomotive field in terms of the field powers and wavelengths, eqs. (20), (21) and eq. (10) are substituted into eq. (4). Then, substituting eq. (18) together with eq. (17) for the beams waist (for the case where $w_{0s} = w_{0w}$) gives a convenient expression for the ponderomotive field:

$$E_{pond} = \frac{4}{\pi}\frac{e}{mc^2}\left(\frac{\mu_0}{\epsilon_0}\right)^{1/2}\left(\frac{\lambda_s}{\lambda_w}\right)^{1/2}\frac{(P_sP_w)^{1/2}}{l_{int}}$$

$$= 0.94 \times 10^{-3}\left(\frac{\lambda_s}{\lambda_w}\right)^{1/2}\frac{(P_sP_w)^{1/2}}{l_{int}}, \tag{22}$$

where the units are in the mks system.

Next, we can fix, according to the condition given in eq. (7), the intensity of the accelerating electric field to be

$$E_{ac} = \tfrac{1}{2}E_{pond}. \tag{23}$$

Using the last equation, together with the assumption of constant axial electric field and eq. (22), the potential drop applied over the interaction length will have the form

$$\Delta\phi = E_{ac}l_{int} = 0.47 \times 10^{-3}\left(\frac{\lambda_s}{\lambda_w}\right)^{1/2}(P_sP_w)^{1/2}. \tag{24}$$

The power that can be generated in this scheme is proportional to the current trapped in the ponderomotive potential wells. Observations of electron trapping by laser beat and energy transfer effect were reported in refs. [10] and [11]. In that experiment, a trapping efficiency of 25% was obtained. A new scheme that injects electrons into the traps by means of an abrupt (non-adiabatic) change in the axial field [12,13] demonstrated a trapping efficiency as high as 60%. In general, we can write, $I_{trap} = \eta I$ where η is the trapping efficiency and I is the current entering the interaction region. The substitution of eq. (24) into the gain equation (13) yields

$$G = 0.47 \times 10^{-3}\left(\frac{\lambda_s}{\lambda_w}\right)^{1/2}\left(\frac{P_w}{P_s}\right)^{1/2} I_{trap}. \tag{25}$$

Clearly, the gain grows in proportion to the current I. However, a large current can produce an effective energy spread across the beam due to the space charge effect ($\Delta\mathscr{E}$ [eV] = $30I$ [A]$/\beta$) which may exceed the trap depth $\mathscr{E}_{trap}$ and not satisfy the inequality (8). The rhs of this inequality can be expressed in terms of power by substituting eqs. (20) and (21):

$$\mathscr{E}_{trap} = 1 \times 10^{-3}\left(\frac{\lambda_w - \lambda_s}{\tau_w}\right)^{1/2}(P_wP_s)^{1/4}. \tag{26}$$

It should be noted that the longitudinal energy spread problem due to the space charge effect can be eliminated if Brillouin flow can be realized in the beam. In this case eq. (8) will be limited by thermal energy spread and emittance.

4. Examples

In this section we present numerical examples, which do not yet correspond to optimized design parameters, in order to demonstrate the possibilities of realizing the proposed scheme. The examples are detailed in tables 1 and 2. In these examples, the pump field is produced by a continuously pulsed high-power CO_2 laser (at 10.6 μm) and a Nd : YAG laser (at 1.06 μm).

The numerical calculation was done for operating the scheme in the 10–100 nm region. In this region, when the CO_2 laser is used as a pump, the required electron energy is 2 MeV at 100 nm ranging up to 8 MeV at 10 nm. Pumping with the Nd : YAG laser reduces this energy range to 0.4–2 MeV. These are very low energies and could be attained by quite compact accelerators – either rf or high-current electrostatic accelerators.

The signal in the 10–100 nm region can be generated by nonlinear frequency mixing. The third- and fifth-order frequency conversion is a straightforward method for producing an XUV seed radiation pulse of narrow spectral width and high intensity (0.03–100 W) [15]. Another method for the production of radiation at soft X-ray wavelengths involves the use of laser-produced plasmas. In this method laser pulses are focused onto steel or other targets to produce plasmas emitting intense soft X-ray radiation [16,17]. It requires further study to find out if this pulsed radiation can be spatially and temporally filtered to produce a sufficiently coherent and intense seed radiation pulse for the FEL amplification process.

Table 1
Examples of pumping with CO_2 laser. The example in brackets refers to realization of a Brillouin flow

Cavity dimensions				
l_{int} [cm]	1.5	1.5	1.5	1.5
L [m]	30	30	30	30
Electron beam				
γ_0	5.2	7.3	9.4	16.3
$\mathscr{E}_e$ [MeV]	2.2	3.2	4.3	7.8
I [A]	3.0	3.0	5.0	5.0 (30)
I_{trap} [A]	0.6	0.6	1.0	1.0 (6)
Pump laser pulse				
P_w [GW]	15	20	30	100
τ_w [ns]	0.1	0.1	0.1	0.1
$\mathscr{E}_w$ [J]	1.5	2.0	3.0	10
λ_w [μm]	10.6	10.6	10.6	10.6
w_{0w} [mm]	0.16	0.16	0.16	0.16
z_{0w} [mm]	7.5	7.5	7.5	7.5
Signal pulse				
P_s [W]	10	5	8	10
τ_s [ns]	200	200	200	200
$\mathscr{E}_s$ [μJ]	2	1	1.6	2
λ_s [Å]	1000	500	300	100
w_{0s} [mm]	0.16	0.16	0.16	0.16
z_{0s} [m]	0.79	1.6	2.6	7.9
Axial electric field				
E_{ac} [kV/m]	1.2	0.69	0.82	0.96
$\Delta\phi$ [V]	17.7	10.2	12.2	14.4
FEL parameters				
E_{pond} [kV/m]	2.4	1.4	1.6	1.9
$\mathscr{E}_{trap}$ [eV]	203	184	230	328
ΔP_s [W]	10.6	6.1	12.2	14.4 (72)
G	1.1	1.2	1.5	1.4 (7)

Table 2
Examples of pumping with Nd:YAG laser. The example in brackets refers to realization of a Brillouin flow

Cavity dimensions				
l_{int} [cm]	1.5	1.5	1.5	1.5
L [m]	30	30	30	30
Electron beam				
γ_0	1.8	2.4	3.1	5.2
$\mathscr{E}_e$ [MeV]	0.4	0.72	1.1	2.2
I [A]	1.8	2.5	2.5	4.0 (30)
I_{trap} [A]	0.36	0.5	0.5	0.8 (6)
Pump laser pulse				
P_w [GW]	3.0	3.5	4.0	5.0
τ_w [ns]	0.1	0.1	0.1	0.1
$\mathscr{E}_w$ [J]	0.3	0.35	0.4	0.5
λ_w [μm]	1.06	1.06	1.06	1.06
w_{0w} [mm]	0.05	0.05	0.05	0.05
z_{0w} [mm]	6.8	7.1	7.3	7.4
Signal pulse				
P_s [W]	10	10	5	5
τ_s [ns]	200	200	200	100
$\mathscr{E}_s$ [μJ]	2	2	1	0.5
λ_s [Å]	1000	500	300	100
w_{0s} [mm]	0.05	0.05	0.05	0.05
z_{0s} [cm]	7.2	15.2	25.8	79.0
Axial electric field				
E_{ac} [kV/m]	1.8	1.3	0.76	0.48
$\Delta\phi$ [V]	25.0	19.0	11.2	7.2
FEL parameters				
E_{pond} [kV/m]	3.7	2.7	1.5	0.97
$\mathscr{E}_{trap}$ [eV]	41.2	44	38.6	41.2
ΔP_s	9.0	9.5	5.6	5.8 (43.5)
G	0.9	1.0	1.1	1.2 (9.0)

Considering the cavity for the XUV signal, we point out an intensive research and development effort for the fabrication of new, efficient optical components, such as mirrors and beam-splitters, for the X-ray laser cavity [18,19]. In general, there are two types of the reflectors to be used. One is the selective multilayer mirror and the other is the broadband concave mirror with sliding modes. The calculated reflectivity for some materials is 10–40% in the 4–40 nm range [20]. The theory of X-ray mirrors was investigated intensively [21–28] and there are no serious technological problems in their production now.

The electron beam must have the same waist as the optical radiation. At such a waist, the current densities requirements are not too high so the space charge effects are negligible. The trapping efficiency is taken to be 20% for the peak current incoming to the interaction region. Higher values of efficiencies will diminish some of the FEL parameters.

The gain is reduced as the wavelength of the injected signal goes deep into the XUV region. This reduction, which is indicated in eq. (25), can be compensated by the pump radiation wavelength. In turn, the latter will restrain the energy spread in the electrons pulse as it appears in eq. (26) and will call for further cold beam.

The length of the ring cavity shown in fig. 1 is consistent with the length of typical accelerators. For $L = 30$ m and a pump pulse of 0.1 ns with a peak power of 50 GW, the cavity will carry 50 MW of circulating power. If the reflection coefficient of the mirrors for the pump radiation is 99.5%, after one round-trip a medium with 2% gain will bring the pump back to the original level. The repetition rate expected in this scheme is very high. This implies pump lasers of very high average power, which are difficult to realize. A possible com-

promise is to inject a pump pulse once during roundstrips so that the output will consist of continuous macropulses.

The energy extraction from the pump power is given by the Manely–Rowe relations, which state that the generation rate of the signal photon flux is equal to the annihilation rate of pump photons, $\Delta P_s/\omega_s = \Delta P_w/\omega_w$ [29]. The total generated signal power ΔP_s is derived from both the pump power ΔP_s is derived from both the pump power ΔP_w and the axial electric power ΔP_{ac}. In the examples given in tables 1 and 2, $\omega_w \ll \omega_s$ and $P_s \ll P_w$, and the pump wave attenuation $\Delta P_w/P_w$ due to the pump depletion can be neglected in comparison with the lasers in the mirrors.

An injected short-wavelength signal laser pulse of the level of several watts may be hard to achieve. However, a low-level XUV seed radiation produced by one of the methods mentioned before can be ramped from low to high signal power level by the FEL amplification process.

References

[1] J. Gea-Banacloche, G.T. Moore, R.R. Schlicher, M.O. Scully and H. Walther, Nucl. Instr. and Meth. A272 (1988) 199.

[2] J. Gea-Banacloche, G.T. Moore, R.R. Schlicher, M.O. Scully and H. Walther, IEEE J. Quantum Electron. QE-23 (1987) 1558.

[3] J.E. La Sala, D.A.G. Deacon and J.M.J. Madey, Proc. SPIE 582 (1986) 156.

[4] B.E. Newnam, J.C. Goldstein, J.S. Fraser and R.K. Cooper, AIP Conf. Proc. 119 (1984) 119.

[5] J.B. Murphy and C. Pellegrini, Nucl. Instr. and Meth. A237 (1985) 159.

[6] M. Billardon, P. Ellaume, J.M. Ortega, C. Bazin, M. Bergher, M. Velghe, D.A.G. Deacon and Y. Petroff, IEEE J. Quantum Electron. QE-21 (1985) 805.

[7] A. Gover, C.M. Tang and P. Sprangle, J. Appl. Phys. 53 (1982) 124.

[8] P. Sprangle and C.M. Tang, AIAA J. 19 (1981) 1164.

[9] A. Yariv, Introduction to Optical Electronics (Holt, Rinehart and Winston, New York, 1976).

[10] R.Z. Olshan, A. Gover, S. Ruschin, H. Kleinman, A. Friedman, B. Stienberg and I. Katz, Nucl. Instr. and Meth. A250 (1986) 244.

[11] R.Z. Olshan, A. Gover, S. Ruschin and H. Kleinman, Phys. Rev. Lett. 58 (1987) 483.

[12] Z. Sheena, S. Ruschin, A. Gover and H. Kleinman, IEEE J. Quantum Electron. QE-26 (1990) 203.

[13] Z. Sheena, S. Ruschin, A. Gover and H. Kleinman, Nucl. Instr. and Meth. A285 (1989) 239.

[14] G.R. Brewer, J. Appl. Phys. 30 (1958) 1022.

[15] R. Hilbig, A. Lago, B. Wolff and R. Wallenstein, Proc. AIP Conf. 147 (1986) 382.

[16] R. Kodama, K. Okada, N. Ikeda, M. Mineo, K.A. Tanaka, T. Mochizuki and C. Yamanaka, J. Appl. Phys. 59 (1986) 3050.

[17] W.C. Mead, E.K. Strover, R.L. Kauffman, H.N. Kornblum and B.F. Lasinski, Phys. Rev. A38 (1985) 5275.

[18] A.M. Hawryluk, N.M. Ceglio and D.G. Stearns, J. Vac. Sci. Technol. B6 (1988) 2153.

[19] N.M. Ceglio, and D.G. Stearns, A.M. Hawryluk, T.W. Barbee, K. Danzmann, M. Kuhne, P. Mueller, B. Wende, M.B. Stearns, A.K. Petford-Long and C.H. Chang, J. Phys. (Paris) C6 (1986) 277.

[20] A.V. Vinogradov, J. Phys. (Paris) C6 (1986) 288.

[21] E. Spiller, Appl. Phys. Lett. 20 (1972) 365; Appl. Opt. 15 (1976) 2333.

[22] A.V. Vinogradov and B.Ya. Zeldovich, Appl. Opt. 16 (1977) 89.

[23] J.H. Underwood and T.W. Barbee, Jr., in: Low Energy X-Ray Diagnostics, eds. D.T. Attwood and B.L. Henke, AIP Conf. Proc. 75 (1981) 170.

[24] S.V. Gaponov, S.A. Gusev, B.M. Luskin and N. Salashchenko, Opt. Commun. 38 (1981) 7.

[25] G.H. Vineyard, Phys. Rev. B26 (1982) 4146.

[26] S.V. Gaponov, F.V. Garin, S.L. Geseu, A.V. Kochemasou, Yu.Ya. Plantonov, N.N. Salashchenko and E.S. Gluskin, Nucl. Instr. and Meth. 208 (1983) 227.

[27] P. Lee, J. Bartlett and D.R. Kania, Opt. Eng. 24 (1985) 197.

[28] T.W. Barbee, Jr., S. Mrowka and M.C. Hettrick, Appl. Opt. 24 (1985) 883.

[29] A. Gover, Opt. Commun. 15 (1983) 281.